*Progress In Electromagnetics Research, Vol. 114, 1–15, 2011*

# ULTRAWIDEBAND ANTENNA EXCITED BY A PHOTOMIXER FOR TERAHERTZ BAND

**B. Andres-Garcia, L. E. Garcia-Muñoz and D. Segovia-Vargas**

Department of Signal Theory and Communications
Radiofrequency Group
Carlos III University of Madrid, 28091, Spain

**I. Camara-Mayorga and R. Güsten**

Max Planck Institute for Radio Astronomy
Bonn 53121, Germany

**Abstract**—An end-fire linear tapered slot antenna is presented in the terahertz band. The operation frequency goes from 0.6 THz to 2 THz, with symmetric radiation patterns from 1 THz to 1.7 THz, and gains up to 15 dB. The gaussicity of the beam is over 80% in the whole operation band and an efficiency at 1 THz of 85%. This antenna gives enough directivity avoiding the use of a typical substrate lens, which introduce 30% of losses. This new design is a good candidate for new applications in the THz range in Radioastronomy and Imaging.

## 1. INTRODUCTION

The terahertz band is still a challenge from the technological point of view. The potential applications which could emerge from the exploitation of this part of the electromagnetic spectrum are considerably limited by the current technology. This fact has led to the coining of the term "THz gap". Approaches from the microwave and photonics have being extensively used to close this gap. In this paper, a design making use of both microwave and photonics techniques is presented: the generation of radiation is performed by a photonic mixer whereas the radiation to free space is accomplished by a tapered slot antenna.

*Received January 25 2011, Accepted 11 February 2011, Scheduled 15 February 2011*
Corresponding author: Belen Andres-Garcia (belens@tsc.uc3m.es).

Photomixing is a well established technique for signal generation in the millimeter and submillimeter bands [1]. The huge bandwidth offered by a single photomixer (from DC to several terahertz) could potentially revolutionize several applications which require large bandwidth and high resolution. The progress made in the material optimization has lead to carrier trapping times below 1 picosecond [2] at moderate bias voltages, which is essential for fabrication of photomixers in the terahertz range.

Usually, photomixers are used to excite a large variety of antennas, both resonant and broadband structures like dipoles, bowties and log-periodic spirals. Due to the insufficient directivity of these antennas, it is often necessary to collimate the beam, using a so-called lens substrate, which usually has an extended-hemispherical form. Another reason for the use of this type of substrate is that no power is lost in surface modes [3]. The substrate with the photomixer device is usually glued to the substrate lens whose dielectric constant is chosen to be similar to that of the photomixer substrate (which is usually a III-V compound semiconductor [4, 5]). This fact avoids reflection in the interface between both media. Nevertheless, since the terahertz beam is collimated in the lens-substrate to free-space interface, power is lost due to the reflection in the interface. Due to the relatively high dielectric constant of the lens-substrate ($\epsilon_r \approx 13$) the reflection losses in this interface are roughly 30%.

Since broadband antireflection coatings in the THz band are difficult to process, specially on curved substrates, it is not easy to avoid the power lost due to reflection losses on the lens-substrate to free-space interface. This fact, together with the complex adjustment of the lens substrate relative to the radiating antenna (coma and spherical aberrations might occur if not properly adjusted) motivated the authors to consider another approach.

In this paper, we propose the design of an antenna removing the substrate lens and preserving all the properties of high directivity, low beamwidth, broadband, high impedance and high gaussicity, with the use of a Tapered Slot Antenna (TSA).

The TSAs have been widely used in the teraherzt band for several applications [6–9]. The preference for this type of antenna arises from its radiation characteristics: symmetric radiation patterns, end-fire radiation, high gain, and also due to the ease in achieving a relatively high input impedance over a large range of frequencies which is beneficial for impedance matching between antenna and generator (photomixer). In addition, this antenna is compatible with planar technology which confers compactness in the construction of arrays — specially of interest for imaging applications and in the use as feeding

of reflectors [10]. These properties make a design based on a TSA very attracting for some astronomical applications, or for imaging arrays, where the spacing between pixels is of special relevance in order to achieve the proper spatial resolution. Nevertheless, the use of planar technology has a strong physical limitation in the terahertz band, due to the lack of very thin and robust substrates that give low effective thickness that can be used to manufacture this antennas.Regarding substrate thickness, the TSAs have special constraints: the substrate should be extremely thin, compared to the wavelength, as reported by [12, 13]. The effective thickness of the substrate must be in the range $(0.005–0.03)\lambda_0$ and it is computed as Eq. (1). For an antenna working in the THz band, this results in a substrate thickness of several microns, which limits seriously its practical implementation.

$$t_{eff} = t(\sqrt{\epsilon_r} - 1) \tag{1}$$

In the last years, there have been some attempts to implement TSAs in the terahertz band [6, 8, 14, 15]. These designs aim to lower the effective thickness of the substrate by modifying geometrical characteristics, so that a thicker substrate can be used to print the antenna, overcoming the limit previously predicted. Other studies try to manufacture the TSAs in extremely thin substrates, as [17], in the 2 THz band. Most of them are resonant structures, that work properly in a narrow bandwidth, not taking advantage of the ultrawideband characteristics of the TSAs as first designed [13, 16].

Also, these studies modify the shape of the TSA or print corrugations in the metallization in order to allow thicker substrates [14, 18]. These are also narrowband approaches, symmetrizing the beam in a narrow bandwidth.

In this paper, the limitation on the substrate thickness is overcome, by using a new geometry for the substrate. The ultrawideband characteristics are maintained and the symmetrization of the radiation patterns is achieved in most of the operation bandwidth, with a high gain. The simulations have been carried out with CST Microwave Studio 2008 [19].

The paper is organized as follows: in Section 2, the design constraints and process are described. In Section 3, the feeding region characteristics are shown, while in Section 4 the shape optimization to achieve the desired radiation characteristics is detailed, followed by the study of the beam gaussicity in Section 4.1. Finally, in Section 4, a low frequency prototype manufactured is presented, together with the measurement of the radiation pattern for the structure.

## 2. PROBLEM AND DESIGN PROCESS

### 2.1. Substrate Design

The use of photomixers as exciting elements for antennas involves some mechanical and physical constraints in the antenna design. First of all, photomixers are processed on III-V compound semiconductor substrates ($\epsilon_r \approx 13$), with a typical thickness of several hundreds of microns. When calculating the effective thickness of the substrate (defined as Eq. (1)) results in $1.72\lambda_0$ at 1 THz for a substrate of 200 μm, much higher than the limit predicted in previous studies [12, 13]. As a consequence the substrate prevents the TSA from end-fire radiation.

One could argue that the photomixer substrate might be thinned to few microns in order to fulfill the thickness condition. The thinned photomixer substrate could be then glued on a low dielectric permittivity substrate. Unfortunately, since the photomixer is illuminated by a relatively large optical power (several tens of mW) [5] in an active area of a few microns, in order to optimize thermal flow it is necessary to avoid thermal interfaces in the regions underneath the photomixer (i.e., several microns under the illuminated surface). As a consequence the substrate thinning option should be discarded.

The fact that the photomixer substrate is a III-V compound semiconductor causes an important difficulty for the use of a TSA as a radiating element: it is mandatory to isolate the photomixer and antenna substrates, otherwise the photomixer substrate would act as a substrate of the antenna thereby preventing from end-fire radiation. This constraint can be overcome by processing the TSA over a wedge of a low losses polymer material (Polymethylpentene TPX) with $\epsilon_r = 2.2$ as shown in Fig. 1. Two goals are satisfied with this geometry: first, the wedge acts as a substrate for the TSA and second, it prevents the radiation from the TSA from "seeing" the photomixer substrate.

The elevation angle of the wedge is of special relevance. If this angle is small, the proper isolation from the photomixer substrate is not achieved, being affected by its properties and preventing radiation due to the high effective thickness specially in the high band. Also, a secondary lobe appears due to the radiation over the photomixer substrate. On the other hand, if the elevation angle is large, the thickness of the TSA substrate becomes higher, also preventing radiation of the TSA. If the elevation angle is near 90°, the thickness of the substrate tends to the previously explained limit, but due to the excitation of the photomixer, that is performed by a pigtailed optical fiber, blockage and perturbations on the radiation pattern might occur, since the radiation diagram will be pointing in the direction of the optical fiber.

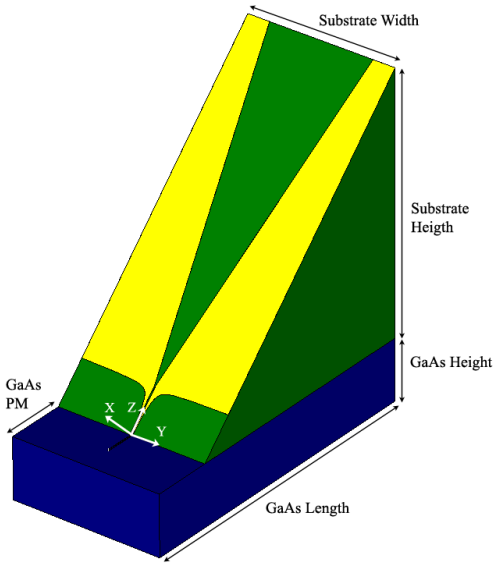


**Figure 1.** Complete structure.

The chosen elevation angle for the wedge substrate is 45°. With this angle, the radiation patterns with the lowest Side Lobe Level (SLL), highest directivity and lowest misalignment of the main lobe depending on frequency are achieved over a wider bandwidth according to the simulations. With this elevation angle, within the TSA radiating area, the $t_{eff}$ ranges from $0.17\lambda_0$ (50, 7 mm) to $1.4\lambda_0$ (408, 3 mm), which in fact exceeds in a factor between 50 and 1000 times the limitation stated before. Clearly, due to this novel design, the substrate thickness limitation has been overcome, making it possible the practical manufacturing of a photomixer fed tapered slot antennas at terahertz frequencies.

## 2.2. Structure Overview and Design Proccess

Once the substrate effective thickness limitation has been solved, some design issues arise due to the characteristics of the technology employed. First of all, due to the different antenna and photomixer substrates, it is necessary to design a feeding region that maximizes the energy flow from the generator to the antenna. In addition to the maximization of the energy delivered to the antenna: since photomixers have input impedance of the order of several $k\Omega$, it is desirable to achieve an input impedance as high as possible.

The geometry chosen for the feeding region determines the input impedance and the energy delivered to the TSA. The shape of the

feeding region has an influence over the radiation characteristics of the antenna. Fine adjustments in the geometric parameters of the feeding region have no significant influence on the radiation pattern. The constraints for the design of this region are the angle of the wedge where the TSA is printed, and the requirements of the photomixer (detailed in Section 3).

## 3. FEEDING REGION DESIGN

The illumination of the photomixer is performed by a single mode fiber optic which is pigtailed to the photomixer by an optical UV curing adhesive. The fiber optic contains the two wavelengths whose difference frequency is generated in the photomixer. The dimensions of the fiber impose a limitation on the distance at which the wedge must be placed from the photomixer: at least a distance equal to the radius of the optical fiber.

The high photomixer impedance causes a mismatch when coupling to antenna, which has an input impedance of hundreds of ohms. Due to this reason, the design of the feeding region must be accomplished according with this characteristic. The typical input impedance of a tapered slot antenna depends on the geometry of the feeding region and also on the substrate dielectric constant and effective thickness [20], and is around $200\,\Omega$, so the highest possible input impedance must be achieved, preserving the radiation characteristics of the antenna in order to have the lowest possible mismatch. In addition, an optimal transition in the coplanar strip (CPS) transmission line should be designed for coupling the power from the CPS on the photomixer substrate to the CPS on the TSA substrate. Regarding the practical manufacturing of this transition, due to alignment purposes between both CPS, a minimum metallization width of $3\,\mu m$ has been considered.

### 3.1. GaAs Transmission Line

In order to ease the CPS transmission line transition, a taper has been implemented in the CPS coming from the photomixer substrate. This taper structure minimizes the losses and at the same time the radiation efficiency and TSA input impedance are maximized.

The design of the transmission line on the photomixer substrate will limit the radiation efficiency of the antenna due to radiation losses, so it is desirable that length of the transmission line is maintained as short as possible. As stated before, the photomixer pigtail imposes a minimum length for the CPS transmission line equal to one radius

of the fiber (62.5 μm). In order to have some margin and since due to capillarity the optical adhesive smears out several tens of microns around of the pigtail position we took 100 μm for the CPS transmission line length (see Fig. 2). Usually, for a CPS transmission line, the lower the gap between lines and the lower the line width, the higher the characteristic impedance of the line [21], nevertheless, for this application, is necessary to design the CPS also paying attention to the high radiation losses, which lower the radiation efficiency of the structure.

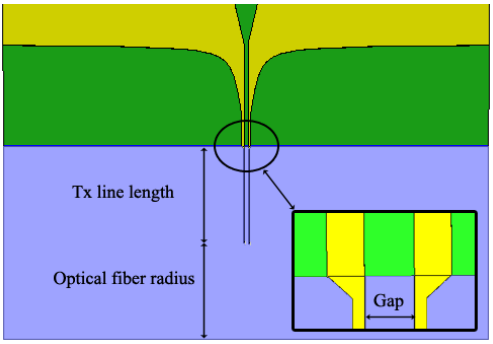


**Figure 2.** Detail of the feeding region. Tx line length = 100 μm, Optical fiber radius = 100 μm.

A parametric study of the two free design parameters of the CPS has been carried out. The gap and the line width, were chosen in order to: first, minimize the losses on the substrate and second, to maximize the input impedance. Fig. 3 shows both parameters in terms of the frequency and the variation of both the gap and the line width. In both figures, the radiation efficiency is shown for the whole structure (CPS and TSA) and for only the portion of the structure on wedge substrate. For this study, a constant linewidth was employed, i.e., same linewidth for both the CPS photomixer substrate and the wedge substrate.

When considering the TSA without the CPS on the photomixer substrate, it is clear from Fig. 3 that changes in the line width and the gap of the CPS on the wedge substrate have almost no influence on the radiation efficiency — which lies over 80% in almost the whole band. When simulating the structure with both substrates, the line width and the gap play a major role in the radiation efficiency, since these parameters determine the radiation losses in the CPS on the photomixer substrate.

As the gap decreases, the input impedance increases [21]. A minimum gap has been chosen which preserves the efficiency. With a

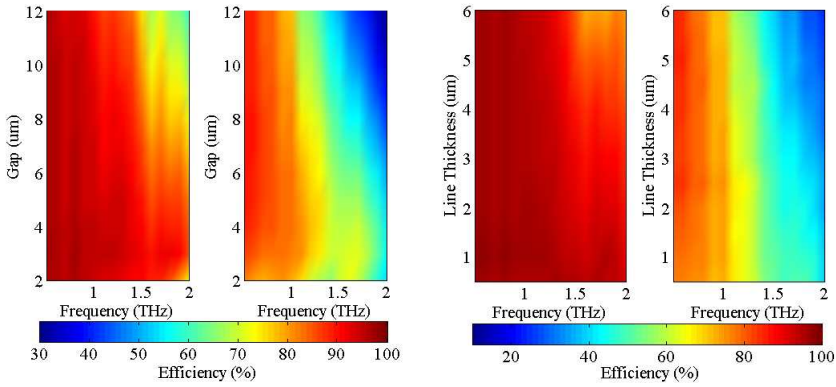


**Figure 3.** (a) Radiation efficiency in terms of frequency, for the whole structure (right) and for the LTSA over the plastic substrate only (left) for (a) gap variation and (b) line width variation.

**Table 1.** Feeding region parameters.

| Parameter | Value (μm) |
|---|---|
| Line Gap | 4 |
| Line Width GaAs | 1 |
| Line Width Substrate | 3 |
| Transmission line length in GaAs | 100 |
| Optical fiber radius | 100 |

gap of 4 μm, the input impedance is maximized whereas the radiation losses over the maximum bandwidth are minimized. The radiation characteristics of the antenna are maintained.

Regarding the line width, it should remain as thin as possible. The width of the CPS lines on the photomixer substrate has been chosen to be 1 μm. Smaller values influence negatively the yield in the lithographic process and might trigger electromigration. As explained before, there should be a minimum width of 3 μm in the transmission line on the junction between CPS on the photomixer and wedge substrates. This has been achieved by including a taper (see Fig. 2) in the last section of the CPS on the photomixer substrate.

A constant width line can not be applied to this design due to the high losses and the low input impedance that result, especially in the high band.

The details of the feeding region are shown in Fig. 2. The relevant parameters are listed in Table 1.

### 3.2. Substrate Transition from CPS Transmission Line to TSA

In order to provide a soft transition from the CPS to the TSA, a tangential shape has been employed. The curve defining this shape is given by Eq. (2).

$$y = \frac{Taper\ Width}{\frac{\pi}{2}} \text{arctg} \frac{x - gap - Tx\ line\ width}{Smoothing\ factor} \tag{2}$$

where the smoothing factor in the denominator corresponds to the profile of the taper. If the smoothing factor is low, the transition from the line to the TSA becomes more abrupt. This factor has been optimized in order to minimize the losses and maximize the radiation efficiency.

### 3.3. Input Impedance

With the parameters detailed in the previous section, the input impedance of the TSA over the operation bandwidth is shown in Fig. 4. The real part is between 150 Ω and 50 Ω, over the whole operation band, being 100 Ω at the central frequency. This input impedance is two orders of magnitude below the output impedance of the photomixer. Regarding the imaginary part, it oscillates around 0 Ω, which is typical for this type of antennas.

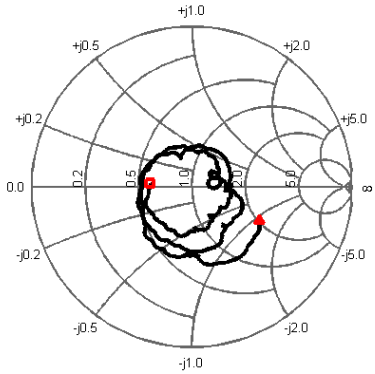


**Figure 4.** $S_{11}$ parameter normalized to 75 Ω. Ending point: 2 THz (square), Starting point: 0.6 THz (triangle).

## 4. SHAPE OPTIMIZATION

Once the feeding region is designed, the remaining parameters correspond to the shape of the antenna. These parameters define only the radiation characteristics of the TSA and do not have any influence over the input impedance, which is determined by the feeding region.

The main goals for the shape optimization are: maximum operation bandwidth, symmetrization of the radiation patterns in the maximum possible bandwidth and achieve the maximum gain in the operation frequency band.

For optimizing the gain, a linear shape for the TSA has been selected [13]. The remaining goals are achieved with the optimization of the parameters of the LTSA, as the length, aperture angle and total width. With these parameters, the frequency range of operation is set up, and also the main characteristics of the radiation patterns, as the $-3$ dB beamwidth, and the minimization of the SLL.

The length of the LTSA ($3.5\lambda_0$) has been chosen by optimizing the operation on the widest frequency range possible, including 1 THz as a central frequency. With this length, the lowest secondary lobes, specially in the $H$ plane are achieved.

The aperture width is set to $1.17\lambda_0$ and the total width (substrate width in Fig. 1) to $1.67\lambda_0$. These last two values also set up the operation band of the TSA. If the aperture angle is reduced, the operation frequency band shifts to upper frequencies [13]. All the design parameters are listed in Table 2, for the shape of the antenna.

**Table 2.** LTSA parameters.

| Parameter | Value |
|---|---|
| Length | $3.5\lambda_0$ |
| Aperture angle | $19^\circ$ |
| Total width | $1.67\lambda_0$ |
| Substrate height | $2.8\lambda_0$ |
| GaAs height | $200\,\mu$m |
| GaAs length | $3.5\lambda_0$ |
| GaAs PM | $200\,\mu$m |

Symmetric radiation patterns at $-3$ dB levels have been achieved from 1 THz to 1.8 THz. In Fig. 5, the radiation patterns at four of these frequencies are shown. The $-3$ dB beamwidths for both main planes of the antenna in the whole operation band are shown in Fig. 6(a).

These beamwidths can be modified by adjusting the shape of the TSA according to [13]. This design achieves one octave with a broadband symmetric radiation pattern, (ranging from 0.9–1.8 THz). There is an asymmetry in the $H$ plane in the radiation patterns. This asymmetry arises from the thickness of the wedge substrate. It produces a secondary lobe in the high band of the antenna. Nevertheless, it remains below $-5$ dB in the whole operation band.

The gain of the antenna is shown in Fig. 6(b), whose maximum is 14.2 dB at 1 THz. The radiation efficiency is also shown, and it has been optimized as explained in Section 2 with the feeding region parameters for 1 THz.

The operation frequency band goes from 0.6 THz to 2 THz with end-fire radiation patterns. These upper and lower limits are given by the shape (i.e., the aperture angle), due to the worse radiation characteristics. The frequency range of operation is set up with these parameters in order to achieve symmetric end-fire radiation patterns, both in the high and in the lower band.

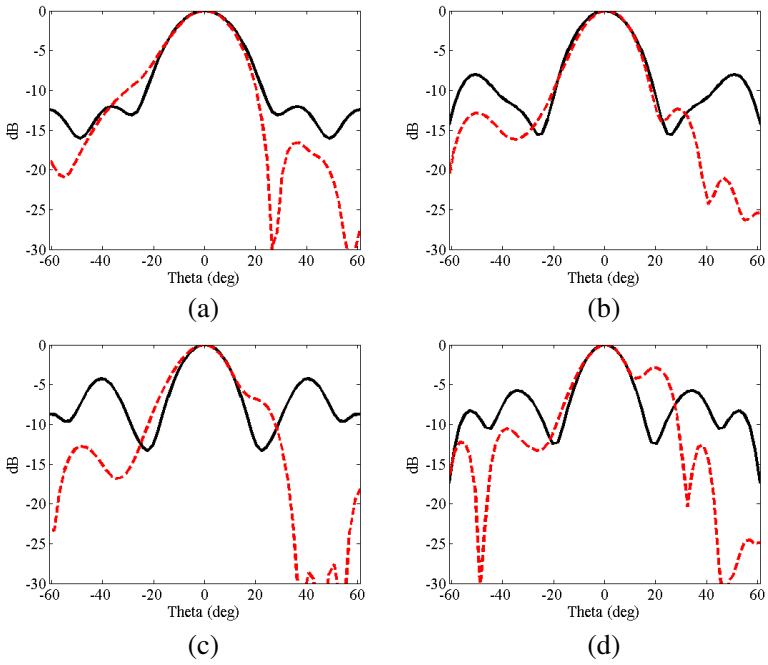


**Figure 5.** Normalized radiation patterns for the $E$ (solid) and $H$ (dashed) planes. (a) 1 THz, (b) 1.2 THz, (c) 1.4 THz and (d) 1.6 THz.

### 4.1. Gaussicity

At terahertz frequencies, the use of the Quasioptical approach is important in terms of the system design. The gaussicity of the antenna is analyzed as defined by [22, 23]. The coupling efficiency is defined as the inner product between the radiation pattern and the fundamental gaussian-beam pattern in the angular domain. The results for this efficiency are shown in Fig. 7. The gaussicity of the beam is over 85% for the whole operation frequency band. The maximum value is achieved at 1.1 THz with 93% gaussicity, agreeing with the maximum gain and symmetrical patterns frequencies.

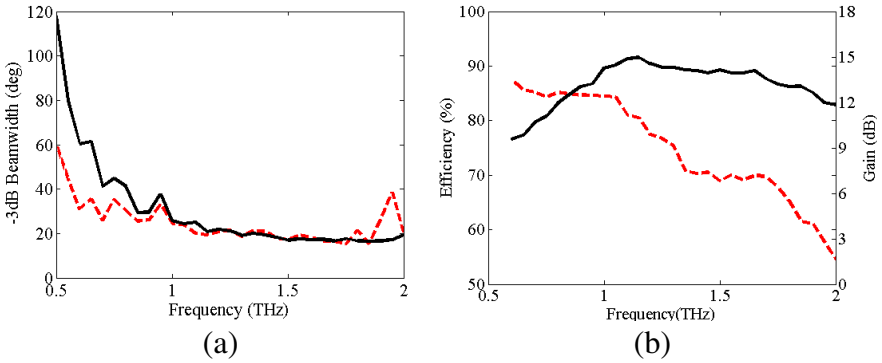


**Figure 6.** (a) $-3$ dB beam widths for the $E$ (solid) and $H$ (dashed) planes in terms of the operation frequency and b) Radiation efficiency (dashed) and Gain (solid) in terms of the frequency.

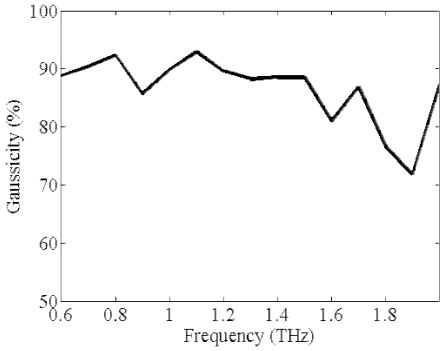


**Figure 7.** Gaussicity for the different operation frequencies.

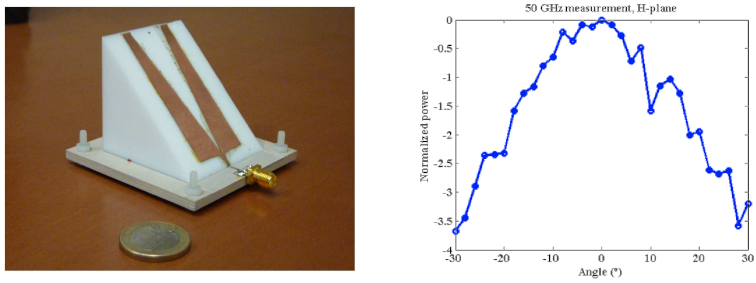


(a) (b)

**Figure 8.** (a) 50 GHz prototype manufactured and (b) radiation $H$-plane measurement.

## 5. LOW FREQUENCY PROTOTYPE

A low frequency prototype has been manufactured with a central frequency of 50 GHz in detection regime. A schottky diode has been employed for detection.

The measurements have been made in an anecoich chamber, measuring the DC power received when transmitting at 50 GHz. Due to the rotational system employed for measurement, only the $H$-plane has been measured, showing the results in Fig. 8.

## 6. CONCLUSION

In this paper, an endfire TSA excited by a photomixer has been designed. Two technologies, microwave and photonics have been employed for the design. With the TSA design, previous theoretical limitations regarding the substrate thickness have been solved, making it feasible the practical manufacturing of high gain antennas in the terahertz band. Symmetric endfire radiation patterns have been achieved, in a frequency band of 0.7 THz, and total operation frequency of 1.5 THz. The gaussicity of the radiation patterns is over 85% in the whole bandwidth. Due to the linear shape used for the TSA design, a maximum gain is accomplished. A feeding region has been also designed maximizing the energy flow from the photomixer to the antenna.

## ACKNOWLEDGMENT

The authors would like to thank to the Max Planck Institute for Radioastronomy for their support in the development of this work. This work has been supported by the projects CAM 2009/00150/001, TERASENSE 2008/00494/001, NeoImag CICYT 2009.

## REFERENCES


1. Brown, E. R., F. W. Smith, and K. A. McIntosh, "Coherent millimeter-wave generation by heterodyne conversion in low-temperature-grown GaAs photoconductors," *Journal of Applied Physics*, Vol. 73, 1480–1484, 1993.
2. Gregory, I. S., C. Baker, W. R. Tribe, M. J. Evans, H. E. Beere, E. H. Linfield, A. G. Davies, and M. Missous, "High resistivity annealed low-temperature GaAs with 100 fs lifetimes," *Journal of Applied Physics*, Vol. 83, 4199, 2003.
3. Rutledge, D. B., D. P. Neikirk, and D. P. Kasilingam, *Infrared and Millimeter Wave*, K. J. Button, Ed., Vol. 10, 1–90, Academic, New York, 1983.
4. Cámara Mayorga, I., P. Muñoz Pradas, E. A. Michael, M. Mikulics, A. Schmitz, P. van der Wal, C. Kaseman, R. Güsten, K. Jacobs, M. Marso, H. Lüth, and P. Kordoš, "Terahertz photonic mixers as local oscillators for hot electron bolometer and superconductor-insulator-superconductor astronomical receivers," *Journal of Applied Physics*, Vol. 100, 3316–3319, 2006.
5. Cámara Mayorga, I., E. A. Michael, A. Schmitz, P. van der Wal, R. Güsten, K. Maier, and A. Dewald, "Terahertz photomixing in high energy oxygen- and nitrogen-ion-implanted GaAs," *Applied Physics Letters*, Vol. 91, 1107–1109, 2007.
6. Ellis, T. J. and G. M. Rebeiz, "MM-wave tapered slot antennas on micromachined photonic bandgap dielectrics," *IEEE MTT-S International Microwave Symposium Digest,* Vol. 2, 1157–1160, Jun. 1996.
7. Lin, S., S. Yang, A. E. Fathy, and A. Elsherbini, "Development of a novel UWB vivaldi antenna array using SIW technology," *Progress In Electromagnetics Research*, Vol. 90, 369–384, 2009.
8. Sigfrid Yngvesson, K., T. L. Korzeniowski, Y.-S. Kim, E. L. Kollberg, and J. F. Johansson, "The tapered slot antenna-A new integrated element for millimeter-wave applications," *IEEE Trans. Microwave Theory Tech.*, Vol. 37, No. 2, Feb. 1989.
9. Yang, Y., Y. Wang, and A. E. Fathy, "Design of compact vivaldi antenna arrays for UWB see through wall applications," *Progress In Electromagnetics Research*, Vol. 82, 401–418, 2008.
10. Conceicao, R. C., M. O'Halloran, M. Glavin, and E. Jones, "Comparison of planar and circular antenna configurations for breast cancer detection using microwave imaging," *Progress In Electromagnetics Research*, Vol. 99, 1–20, 2009.
11. O'Halloran, M., M. Glavin, and E. Jones, "Rotating antenna

microwave imaging system for breast cancer detection," *Progress In Electromagnetics Research*, Vol. 107, 203–217, 2010.

12. Janaswamy, R. and D. H. Schaubert, "Analysis of the tapered slot antenna," *IEEE Trans. Antennas Propag.* Vol. 35, 1058–1065, Sep. 1987.
13. Sigfrid Yngvesson, K., D. H. Shaubert, T. L. Korzeniowski, E. L. Kollberg, T. Thungren, and J. F. Johanson, "Endfire tapered slot antennas on dielectric substrates," *IEEE Trans. Antennas Propag.*, Vol. 33, 1392–1400, Dec. 1985.
14. Rizk, J. B. and G. M. Rebeiz, "Millimeter-wave fermi tapered slot antennas on micromachined silicon substrates," *IEEE Trans. Antennas Propag.*, Vol. 50, No. 3, 379–383, Mar. 2002.
15. Acharya, P. R., H. Ekstrom, S. S. Gearhart, S. Jacobson, J. F. Johansson, E. L. Kollberg, and G. M. Rebeiz, "Tapered slotline antennas at 802 GHz," *IEEE Trans. Microwave Theory Tech.*, Vol. 41, No. 10, 1715–1719, Oct. 1993.
16. Mehdipour, A., K. Mohammadpour-Aghdam, and R. Fara Ji-Dana, "Complete dispersion analysis of vivaldi antenna for ultra wideband applications," *Progress In Electromagnetics Research*, Vol. 77, 85–96, 2007.
17. Svechnikov, S. I., O. V. Okunev, P. A. Yagoubov, G. N. Gol'tsman, E. Gerecht, C. F. Musante, Z. Wang, and K. S. Yngvesson, "2.5 THz NbN hot electron mixer with integrated tapered slot antenna," *IEEE Trans. on Applied Superconductivity*, Vol. 7, No. 2, 3548–3551, Jun. 1997.
18. Sugawara, S., Y. Maita, K. Adachi, K. Mori, and K. Mizuno, "Characteristics of a MM-Wave tapered slot antenna with corrugated edges," *IEEE MTT-S International Microwave Symposium Digest,* Vol. 2, 533–536, Jun. 1998.
19. CST Microwave Studio, 2008.
20. Janaswamy, R. and D. H. Schaubert, "Characteristic impedance of a wide slotline on low-permittivity substrates," *IEEE Trans. Microwave Theory Tech.*, Vol. 34, No. 8, 900–902, Aug. 1986.
21. Simons, R. N., *Coplanar Waveguide Circuits, Components, and Systems*, 1st edition, John Wiley & Sons Inc., New York, US, 2001.
22. Filipovic, D. F., S. S. Gearhart, and G. M. Rebeiz, "Double-slot antennas on extended hemispherical and elliptical silicon dielectric lenses," *IEEE Trans. Microwave Theory Tech.*, Vol. 41, No. 10, 1738–1749, Oct. 1993.
23. Schwarz, S. E., "Efficiency of quasi-optical couplers," *Int. J. Infrared Millimeter Waves*, Vol. 5, No. 12, 321–325, 1984.